

Article

Analysis and Design of Helmholtz Protector to Improve High-Frequency Response of Insert Earphone

Yuan-Wu Jiang ¹, Dan-Ping Xu ², Zhi-Xiong Jiang ¹, Jun-Hyung Kim ¹ and Sang-Moon Hwang ^{1,*} 

¹ School of Mechanical Engineering, Pusan National University, Busan 46241, Korea; evan.jiang.pnu@gmail.com (Y.-W.J.); jzx20180902@gmail.com (Z.-X.J.); joonyng7@gmail.com (J.-H.K.)

² School of Mechatronic Engineering and Automation, Shanghai University, Shanghai 200444, China; sallyxu@gmail.com

* Correspondence: shwang@pusan.ac.kr

Received: 22 April 2019; Accepted: 11 June 2019; Published: 21 June 2019



Abstract: With the development of multimedia devices, earphones are playing an increasingly important role. This article applies the lumped parameter method using an equivalent circuit to model the electromagnetic, mechanical, and acoustic domains of earphones. Then, parameters are determined according to the dimensions and material properties of earphone parts. On the basis of the analysis tool and determined parameters, a Helmholtz protector is analyzed and designed to improve the high-frequency response. Samples are fabricated, and the experiment verifies the analysis method. The experimental result shows that the peaks at 7 k and 10 k are decreased at 8.05 dB and 7.89 dB. The root means square value of SPL deviation compared with target curve decreased from 9.77 to 4.39. High-frequency response is improved by using the Helmholtz protector.

Keywords: earphone; Helmholtz protector; high-frequency response

1. Introduction

With the rapid development of consumer products such as mobile phones, notebook computers, and MP4 players, earphones have been recognized as multifunctional assets to increase the convenience of consumer electronics. Based on the speaker driver type, there are MEMS speaker driver earphones [1], balanced armature speaker driver earphones [2], and dynamic speaker driver earphones [3].

The present study focuses on dynamic speaker driver earphones. The earphone parts are shown in Figure 1. The Lorenz force is generated with an input current in the magnetic circuit. Then, the force contributes to the vibration of the diaphragm, which leads to sound radiation through the front chamber.

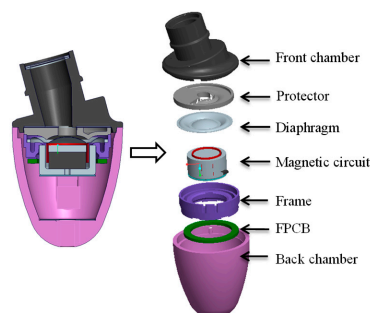


Figure 1. Section view of earphone.

To design and develop the earphone product, some previous studies have presented simulation methods. The finite element method has been used to analyze earphone performance [4]. According to the relationship between multi physics (electromagnetic, mechanical, and acoustic domains) and an equivalent circuit [5,6], the lumped parameter method (LPM) can be used to analyze earphone performance [7,8]. Based on the LPM, coupling between the headphone and the ear has been investigated in artificial ears and models. The influence of the back volume is taken into account [9]. A model of a dynamic driver in an enclosure has been developed using lumped-parameter analysis and analogous circuits [10]. In addition, the properties of porous materials have been investigated to determine their influence on the SPL of an insert earphone [11]. The acoustic structure (volume of front chamber, volume of back chamber duct radius, and length) has been optimized by making use of annealing optimization [12]. To determine the performance of an insert earphone, the target curve for an insert earphone has been defined [13,14].

The parameters of the dynamic speaker driver in previous studies [5–12] were obtained from experiments, so that it is impossible to use these parameters to design a new earphone structure without samples. The first novelty of the present work is the identification of parameters in the analysis tool with respect to the dimensions and material properties. In this way, each dimension and each material property of an earphone can be varied to determine their influence on earphone performance. The second novelty involves analysis and design of a Helmholtz protector based on the proposed analysis tool and identified parameters. It is a challenge to match with the target curve from 7 k to 10 k because the mismatch is generated by the resonance of the ear canal. In other words, they will always exist if there is an ear canal. The paper focuses on the high-frequency response improvement from 7 k to 10 k by reducing the mismatch caused by the ear canal. The designed Helmholtz protector can reduce the peak value of SPL from 7 k to 10 k and improve the earphone high-frequency response.

The main content of this paper is as follows. First, the electromagnetic, mechanical, and acoustic domains are described by the LPM, which makes use of an equivalent circuit. Second, based on the dimensions and material properties, the electromagnetic and mechanical domain parameters are identified by FEM. The acoustic parameters are determined from the acoustic component dimension. These parameters are treated as input information for simulation. Then, based on the simulation, a Helmholtz protector is designed and simulated to improve the SPL. Finally, the earphone sample is manufactured. The SPL simulation result is matched with the experimental result. With the use of a Helmholtz protector, the high-frequency response is improved.

2. Analysis Method

2.1. Electromagnetic Modeling

The electromagnetic part is depicted in Figure 2. The relevant mathematical equation is as follows.

$$Z_E = R_E + j\omega L_E \quad (1)$$

where R_E is the electrical voice coil resistance at DC, L_E is the voice coil inductance, ω is the angular frequency and Z_E is the electrical impedance.



Figure 2. Equivalent circuit of electromagnetic domain.

2.2. Mechanical Modeling

A 1-DOF vibration system is adopted for the mechanical domain, as depicted in Figure 3.

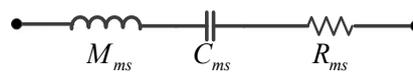


Figure 3. Equivalent circuit of mechanical domain.

The governing equation is as follows.

$$F = M_{ms}\ddot{X} + R_{ms}\dot{X} + \frac{1}{C_{ms}}X \tag{2}$$

where M_{ms} is the mechanical mass of the driver vibration system, R_{ms} is the mechanical resistance of the total-driver losses, C_{ms} is the mechanical compliance of the driver vibration system, and X is displacement.

2.3. Acoustic Modeling

To analyze the SPL performance of an earphone, all acoustic components need to be modeled in the analysis tool. The acoustic domain is modeled as follows.

The acoustic components of a dynamic speaker unit are shown in Figure 4. There is a hole located in the center of the protector. As a result of the existence of a diaphragm, there is a front cavity and a back cavity in the unit. On the yoke, there are three holes.

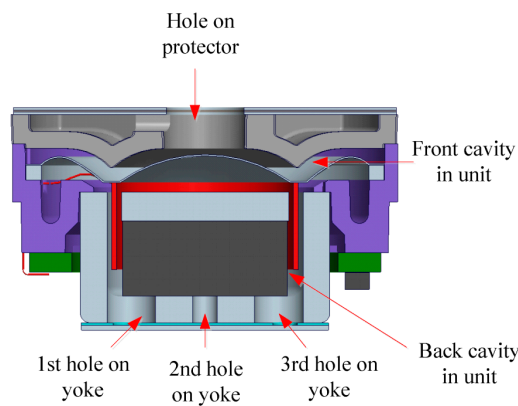


Figure 4. Cavity and hole in dynamic speaker unit.

The cavity is modeled as the acoustical compliance shown in Figure 5.

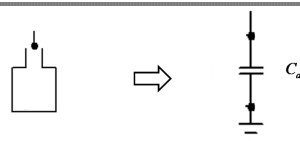


Figure 5. Cavity model and its equivalent circuit.

The related equation to define the acoustical compliance is as follows [15].

$$C_a = \frac{V}{\rho c^2} \tag{3}$$

The small hole is modeled in Figure 6.

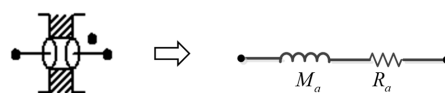


Figure 6. Hole model and its equivalent circuit.

The mathematical expression for the small hole is described by the following equation:

$$Z_{hole} = j\omega M_a + R_a \tag{4}$$

where Z_{hole} , M_a and R_a are the acoustical impedance, acoustical mass and acoustical resistance, respectively, which can be expressed as [16]:

$$M_a = \frac{332-13x+7x^2+2x^3}{249-9x+4x^2+2x^3} \frac{4\rho l}{\pi d^2}$$

$$R_a = 8f\rho l \frac{\sqrt[4]{4096+45x^3+4x^4}}{d^2 x^2} \tag{5}$$

where $x = d/2\beta$; $\beta = \sqrt{(\eta/(\rho 2\pi f))}$ is the viscosity coefficient of the fluid ($\eta = 18.6 \times 10^{-6}$ n·s/m² at 20 °C for air); ω is the angular frequency; and l and d are the length and diameter of the hole, respectively.

In addition to the dynamic speaker unit, a sound port and test jig are also present. Figure 7. demonstrates the acoustic structure. The structure consists of one back chamber, one conical tube, three cylinder tubes, and an IEC-60711 coupler.

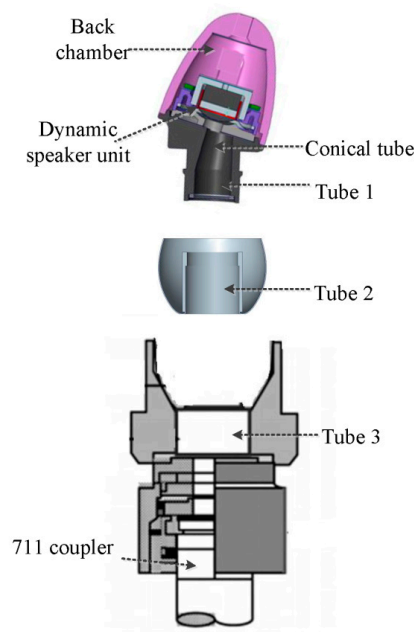


Figure 7. Cross-section view of dynamic earphone experiment condition.

The tubes can be treated as transmission line models. Except for the cylinder tube, there is conical tube in front of the speaker unit. The tube modeling is shown in Figure 8.

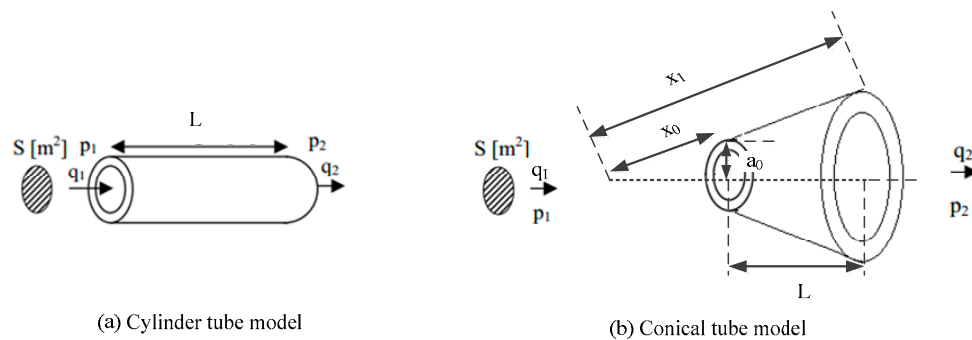


Figure 8. Tube models.

The following equations are mathematic models of a cylinder tube and conical tube.

$$\begin{pmatrix} p_1 \\ q_1 \end{pmatrix} = \begin{bmatrix} \cos(kl) & jZ_w \sin(kl) \\ (j/Z_w) \sin(kl) & \cos(kl) \end{bmatrix} \begin{pmatrix} p_2 \\ q_2 \end{pmatrix} \quad (6)$$

$$\begin{pmatrix} p_1 \\ q_1 \end{pmatrix} = \begin{bmatrix} (\frac{x_1}{x_0}) \cos(kl) - (\frac{1}{kx_0}) \sin(kl) & (\frac{x_0}{x_1}) jZ_w \sin(kl) \\ (\frac{j}{Z_w}) [\frac{x_1}{x_0} + (\frac{1}{kx_0})^2] \sin(kl) - (\frac{L}{x_0}) (\frac{1}{kx_0}) \cos(kl) & (\frac{x_1}{x_0}) [\cos(kl) + (\frac{1}{kx_0}) \sin(kl)] \end{bmatrix} \begin{pmatrix} p_2 \\ q_2 \end{pmatrix}$$

The parameters are $k = \omega/c$, where $\omega = 2\pi f$; $l =$ tube length; and $Z_w = \rho c/S = \rho c/\pi a^2$, where ρ is the air density and c is the speed of sound propagation. $p_1, q_1, p_2,$ and q_2 are inward sound pressure, outward sound pressure, inward volume velocity and outward volume velocity. x_1 and x_0 are the lengths of the tube along the surface direction.

If the diameter of the tube changes, there will be added length because of the existence of radiation impedance at the tube end. The tube end correction is shown in Figure 9.

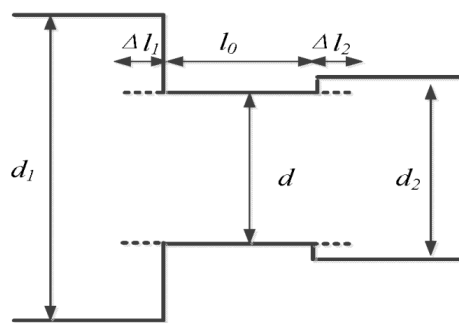


Figure 9. Tube end correction.

The tube end correction is as follows

$$\begin{aligned} \Delta l_1 &= 0.85d [1 - 1.47 \frac{d}{d_1} + 0.47 (\frac{d}{d_1})^3] \\ \Delta l_2 &= 0.85d [1 - 1.47 \frac{d}{d_2} + 0.47 (\frac{d}{d_2})^3] \end{aligned} \quad (7)$$

where $d_1, d, d_2, \Delta l_1, l_0$ and Δl_2 are the left side tube diameter, middle tube diameter, right side tube diameter, left side tube end correction length, middle tube length and right side tube end correction. Considering both sides of the tube end correction

$$l = l_0 + \Delta l_1 + \Delta l_2 \quad (8)$$

The test jig is an IEC-60711 coupler, which is a standard product and has a lumped parameter model [17]. The cross-section view and electrical equivalent circuit are represented in Figure 10. The parameter values are listed in Table 1.

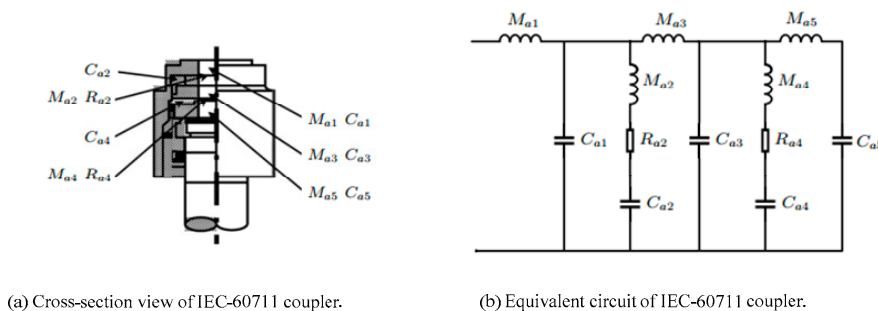


Figure 10. Cross-section view and equivalent circuit of IEC-60711 coupler.

Table 1. Parameters of IEC-60711 coupler.

Item	Value
M_{a1} (kg·m ⁻⁴)	82.9
M_{a2} (kg·m ⁻⁴)	9400
M_{a3} (kg·m ⁻⁴)	130.3
M_{a4} (kg·m ⁻⁴)	983.8
M_{a5} (kg·m ⁻⁴)	133.4
C_{a1} (m ⁵ ·N ⁻¹)	0.943×10^{-12}
C_{a2} (m ⁵ ·N ⁻¹)	1.9×10^{-12}
C_{a3} (m ⁵ ·N ⁻¹)	1.479×10^{-12}
C_{a4} (m ⁵ ·N ⁻¹)	2.1×10^{-12}

2.4. Electromagnetic-Mechanical-Acoustic Coupling

The coupling between the electromagnetic domain and mechanical domain is modeled by current-controlled voltage sources (CCVSs). The model is depicted in Figure 11. In the electromagnetic domain, there is a back EMF, which is determined by the velocity in the mechanical domain. The force in the mechanical domain depends on the current in the electromagnetic domain. The relationships are described by the following equations.

$$\begin{aligned}
 F &= Bli \\
 V_{back} &= Blv
 \end{aligned}
 \tag{9}$$

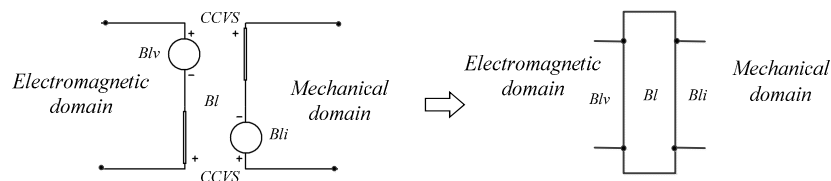


Figure 11. Coupling between electromagnetic and mechanical domains.

Here, F is the force resulting from the current, Bl is the force factor, V_{back} is the back EMF, and v and i are the velocity and current, respectively.

The coupling between the mechanical domain and acoustic domain is modeled by a current-controlled current source (CCCS) and a voltage-controlled voltage source (VCVS). The model is depicted in Figure 12. In the acoustic domain, the volume velocity depends on the velocity in the mechanical domain. The acoustic pressure is determined by the force in the mechanical domain. The relationships are described by the following equations.

$$\begin{aligned}
 p &= \frac{F}{S_d} \\
 V_{volume} &= vS_d
 \end{aligned}
 \tag{10}$$

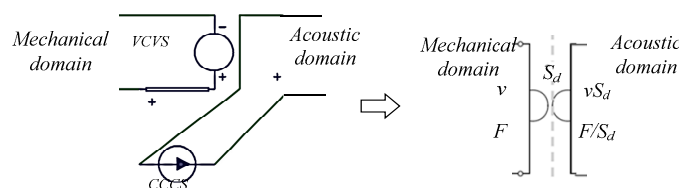


Figure 12. Coupling between mechanical and acoustic domains.

In these equations, p is the acoustic pressure, F is the force in the mechanical domain, S_d is the effective area, and V_{volume} is the volume velocity.

Based on the component circuit model, the equivalent circuit of an earphone is shown Figure 13.

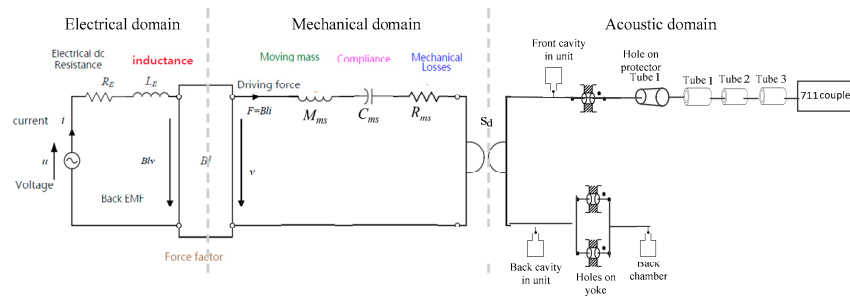


Figure 13. Equivalent circuit of an earphone (without Helmholtz protector).

3. Parameter Identification

3.1. Electromagnetic Parameter Identification

Electromagnetic parameter identification is based on the static magnetic FEM. The boundary condition is shown in Figure 14. The vector potential of the outside air region is zero. The governing equations are

$$\begin{aligned}
 \nabla \times H &= J \\
 B &= \nabla \times A \\
 J &= \sigma E \\
 B &= \mu H
 \end{aligned}
 \tag{11}$$

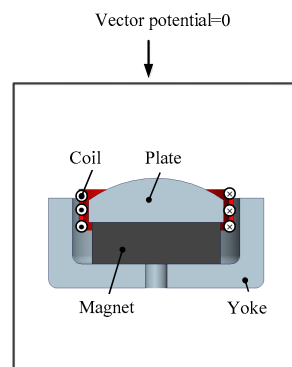


Figure 14. Electromagnetic system model and boundary conditions.

Here, A is the magnetic vector potential, J is the current density, H is the magnetic intensity, μ is the permeability in a vacuum, E is the electric field intensity, and σ is the electrical conductivity. After solving the governing equation, the flux density for every node in the model can be obtained. By solving for the flux density B and flux intensity H , the change in magnetic energy is calculated as

$$\Delta W = \frac{1}{2} \int \Delta H \Delta B dV
 \tag{12}$$

where ΔH and ΔB are the change in magnetic flux intensity and flux density caused by a change in the current. The inductance is related to the change in magnetic energy. The relationship is described as

$$L_E = \frac{2\Delta W}{\Delta I}
 \tag{13}$$

The unit for L_E , ΔW and ΔI are Henry, Joule and Ampere.

3.2. Mechanical Parameter Identification

The mechanical system includes a diaphragm and coil. Figure 15 demonstrates the structure. To determine the mechanical parameters, mechanical FEM simulation is used. The governing equation is as follows

$$[M]\{\ddot{u}\} + [C]\{\dot{u}\} + [K]\{u\} = \{F\} \tag{14}$$

where $[M]$, $[C]$, $[K]$, $\{F\}$, and u denote the mass matrix, damping matrix, stiffness matrix, vector of current force, and displacement, respectively. The boundary conditions are shown in Figure 15. Force is input on the coil. The edge of the diaphragm is fixed. To determine the stiffness, a 0.01-N force is input. The displacement of the coil is 3.598×10^{-2} mm. Then, the stiffness K_{ms} is calculated as the displacement divided by the input force. The resulting value is 0.278 N/mm. By performing modal analysis of the mechanical system, the resonance frequency is found. Based on the relationship between mass, stiffness and resonance frequency

$$f_0 = \frac{1}{2\pi} \sqrt{\frac{K_{ms}}{M_{ms}}} \tag{15}$$

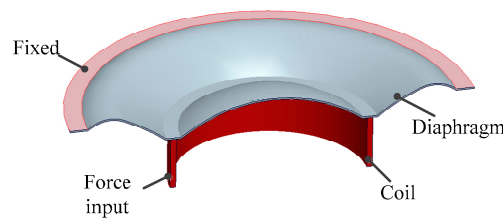


Figure 15. Mechanical system model and boundary conditions.

The mass M_{ms} is calculated as 0.006 g.

Table 2 lists the identified parameters for the dynamic speaker unit.

Table 2. Parameters of dynamic speaker unit.

Item	Value
R_E (Ohm)	15
L_E (mH)	0.02
M_{ms} (g)	0.006
R_{ms} (kg/s)	0.35
C_{ms} (mm/N)	3.597
K_{ms} (N/mm)	0.278

3.3. Acoustic Parameter Identification

The acoustic parameters all relate to the dimensions of the tubes, cavities, and holes. The tube and hole parameters are listed in Table 3. The cavity parameters are given in Table 4.

Table 3. Parameters of holes and tubes.

Item	Length (mm)	Diameter (mm)
1st hole on yoke	0.55	1
2nd hole on yoke	0.55	0.5
3rd hole on yoke	0.55	1
Hole on protector	0.9	1.7
tube 1	2.3	2.5
tube 2	4	2.8
tube 3	6.5	7.4

Table 4. Parameters of cavities.

Item	Value
Front cavity in unit (mm ³)	11.11
Back cavity in unit (mm ³)	25.14
Back chamber (mm ³)	159

3.4. Electromagnetic-Mechanical-Acoustic Coupling Parameter Identification

The electromagnetic-mechanical coupling parameter is the force factor Bl . The flux density is obtained by FEM simulation. With the known coil length, the force factor is calculated to be 0.159 N/A.

The mechanical-acoustic coupling parameter is the effective area of the diaphragm. The method for identifying the effective area is shown in Figure 16.

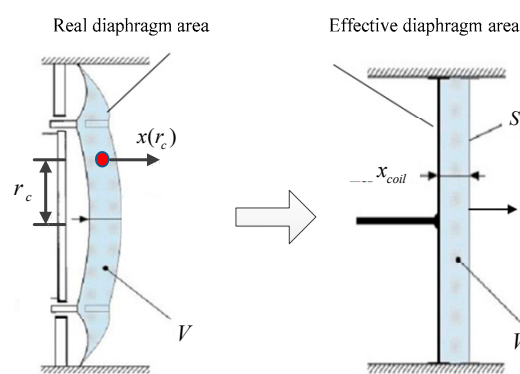


Figure 16. Method for identifying the effective area.

Considering the same air volume V , the effective area is calculated using equation [18].

$$S_d = \frac{\int_{S_c} x(r_c) dS}{x_{coil}} \tag{16}$$

where $x(r_c)$ is the displacement of a point on the diaphragm, r_c is the distance between the point and the center of the diaphragm, and x_{coil} is the average displacement of the coil. To obtain the effective area, the mechanical static FEM is used. The boundary conditions are shown in Figure 17. The input is the displacement of the coil. With fixed boundary conditions and input displacement, the deformation of the diaphragm can be determined. By integrating the deformation on every part of the diaphragm and using the Equation (17), the effective area is calculated to be 28.2 mm².

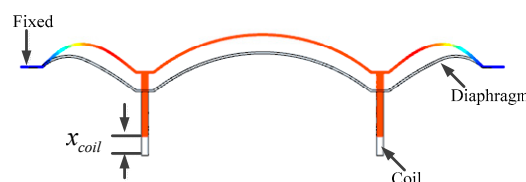


Figure 17. Static analysis to obtain effective area.

After the parameters are applied in the equivalent circuit, the SPL simulation result for an earphone can be obtained. The experiment is performed after the sample is manufactured. According to the SPL comparison of the simulation and experiment in Figure 18, the simulation tool is verified by the experiment and can be used to analyze the performance of a dynamic earphone. From 20 Hz to 7 kHz, the SPL did not decrease because the SPL is tested in the pressure field. The acoustic wave propagates in the front chamber and the IEC-60711 coupler. From 7 kHz to 14 kHz, there are three peaks. The first and second peaks are

due to the front chamber and tubes (ear canal) in the front end. The third peak is due to the IEC-60711 coupler. The experimental and simulation results show that there are differences between the target SPL and the analyzed earphone SPL. In Figure 18, the target comes from previous research by Olive [13,14]. The target curve has the best high-frequency response and can be used as a benchmark.

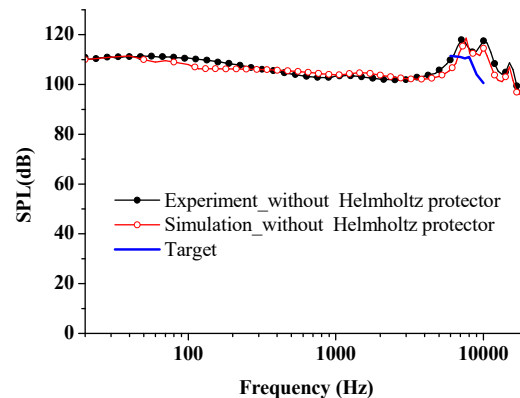


Figure 18. Experimental and simulated results (without Helmholtz protector).

4. Design of Helmholtz Protector

The experimental and simulation results show that there are differences between the target SPL and analyzed earphone SPL. There are two peaks due to the front chamber and tubes (ear canal) in the front end. These two peaks can be decreased using an acoustic structure to decrease the SPL difference between the analyzed earphone and target. In this study, a Helmholtz protector is applied as such an acoustic structure.

The Helmholtz protector consists of two sets of cavities and holes, as shown in Figure 19. The cavity is treated as an acoustical compliance. The small hole is treated as an acoustical resistance and acoustical mass. Therefore, there will be two peaks because there are two sets of cavities and holes. The equivalent circuit of the Helmholtz cavity and hole is parallel to the acoustic sound tube that goes to the IEC-60711 coupler. The cavity and hole set can act as a resonant muffler. The acoustical compliance of cavity is given in Equation (3), and the acoustical mass of the hole is described in Equation (5). The volume of the cavity controls the acoustical compliance, and the length controls the acoustical mass. The protector is manufactured by injection molding. The manufacture tolerance is 0.05 mm. The goal is to cause the resonance of the Helmholtz protector to occur at 7 kHz and 10 kHz. The lengths of the 1st and 2nd holes are selected to be 0.65 mm and 1.6 mm, respectively. The volumes of the 1st and 2nd Helmholtz cavities are 9 mm³ and 2.5 mm³, respectively. With the Helmholtz protector, the earphone equivalent circuit is depicted in Figure 20. Figure 21 shows a comparison of the simulation results for an earphone with a Helmholtz protector and an earphone without a Helmholtz protector. The SPL values at 7 kHz and 10 kHz decrease. Not only are the peak values at 7 kHz and 10 kHz decreased, but there is also a decrease in the entire range from 7 kHz to 10 kHz. Thus, the SPL difference is reduced using the Helmholtz protector.

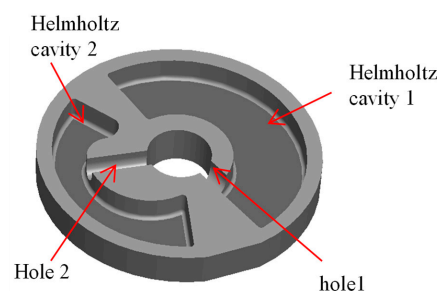


Figure 19. Helmholtz protector geometry.

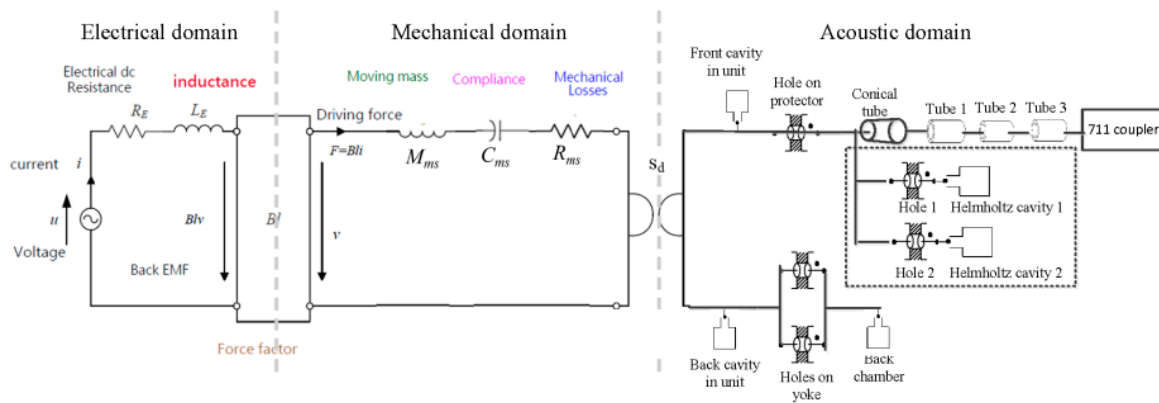


Figure 20. Equivalent circuit of earphone (with Helmholtz protector).

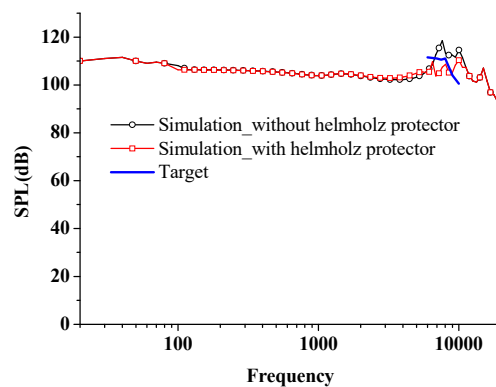


Figure 21. Simulation result (with/without Helmholtz protector).

5. Experiment

To realize this concept, samples were manufactured. Figure 22 demonstrates the sample parts. Figure 23 shows the Helmholtz protector and a normal protector. Figure 24 depicts the equipment and setup for the SPL experiment. In the experiment, an NTI system was applied. The testing frequency range was from 20 Hz to 20 kHz. A swept sine signal was used. In the NTI system, the received sound signal is transformed to the frequency domain by a fast Fourier transform (FFT). Figure 25 shows the experimental SPL results. Just like the comparison of simulation results, the peaks at 7 kHz and 10 kHz are reduced by using the Helmholtz protector. The experimental result for the earphone with the Helmholtz protector shows less difference compared with the earphone without the Helmholtz protector.



Figure 22. Components of dynamic earphone.

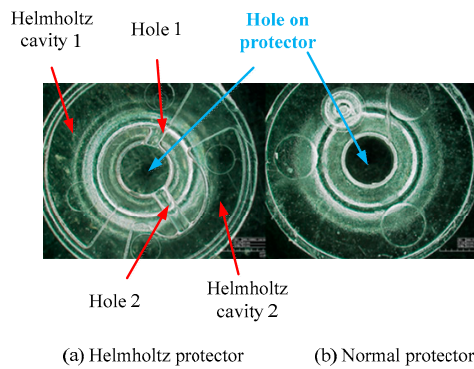


Figure 23. Protector sample.

To check the performance of the earphone from 7 k to 10 k., the root mean square value of SPL deviation is used. The SPL deviation is defined as the SPL difference compared with the target curve [13,14] from 7 k to 10 k. The equation is described as following

$$RMS_{deviation} = \sqrt{\frac{1}{n} \sum_{i=1}^n (y - y_{target})^2}, \tag{17}$$

where y and y_{target} are the SPL value of the designed earphone and target. The root mean square value of the SPL deviation for the earphone with the Helmholtz protector is calculated to be 4.39, while that for the earphone without the Helmholtz protector is 9.77. The high-frequency response is improved when the Helmholtz protector is used.

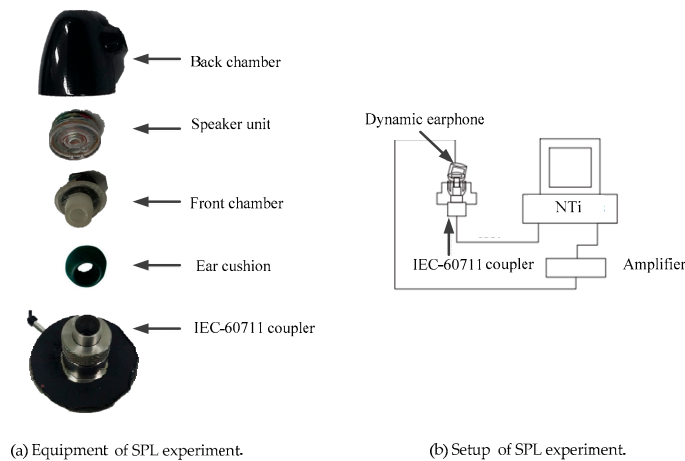


Figure 24. Equipment and setup of sound pressure level (SPL) experiment.

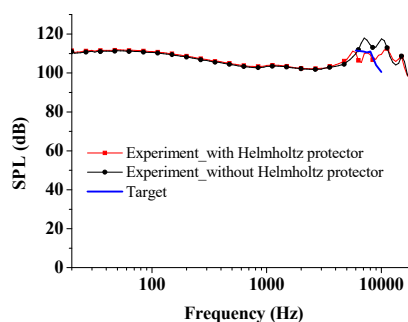


Figure 25. Experimental results (with/without Helmholtz protector).

6. Conclusions

In this study, the dynamic earphone parts are modeled as an electrical element and the equivalent circuit method is used to analyze the SPL. Electromagnetic, mechanical and acoustic parameters are determined based on the earphone parts dimension and material property. According to the SPL analysis method, there are differences between the analyzed earphone SPL and target SPL because of the peaks at 7 kHz and 10 kHz. To decrease the peak value, a Helmholtz protector is designed and applied. The lengths of the 1st and 2nd holes are selected to be 0.65 mm and 1.6 mm, respectively. The volumes of the 1st and 2nd Helmholtz cavities are 9 mm³ and 2.5 mm³, respectively. Samples are manufactured, and experiments are conducted. A comparison shows that the analysis is verified by the experimental result. Furthermore, with the Helmholtz protector, the difference in the SPL is reduced. The root mean square value of the SPL deviation for the earphone with the Helmholtz protector is 4.39, while that for the earphone without the Helmholtz protector is 9.77. The high-frequency response is thus improved using the Helmholtz protector.

Author Contributions: Data curation, Y.-W.J. and J.-H.K.; Formal analysis, Y.-W.J., D.-P.X. and Z.-X.J.; Funding acquisition, S.-M.H.; Investigation, Y.-W.J. and D.-P.X.; Methodology, Y.-W.J. and D.-P.X.; Project administration, Y.-W.J. and S.-M.H.; Resources, Y.-W.J. and D.-P.X.; Software, Z.-X.J. and J.-H.K.

Funding: This research received no external funding

Conflicts of Interest: The authors declare no conflict of interest.

Abbreviations

The following abbreviations are used in this manuscript:

SPL	Sound pressure level
MEMS	Micro-Electro-Mechanical System
HATS	Head and Torso Simulator
FFT	Fast Fourier Transform

References

- Männchen, A.; Stoppel, F.; Beer, D.; Niekkel, F.; Wagner, B. In-ear headphone system with piezoelectric mems driver. In Proceedings of the 145th Audio Engineering Society Convention, New York, NY, USA, 17–20 October 2018.
- Jiang, Y.W.; Xu, D.P.; Hwang, S.M. Electromagnetic-mechanical analysis of a balanced armature receiver by considering the nonlinear parameters as a function of displacement and current. *IEEE Trans. Magn.* **2018**, *99*, 1–4.
- White, J. Considerations in high-fidelity moving-coil earphone design. *IEEE Trans. Audio* **1963**, *6*, 188–194. [[CrossRef](#)]
- Biba, D.; Opitz, M. Development of a finite element headphone model. In Proceedings of the 122nd Audio Engineering Society Convention, Vienna, Austria, 5–8 May 2007.
- Bauer, B.B. Equivalent circuit analysis of mechano-acoustic structures. *J. Audio Eng. Soc.* **1976**, *24*, 643–652.
- Leach, W.M., Jr. Analogous circuits for acoustical systems and analogous circuits for mechanical systems. In *Introduction to Electroacoustic and Audio Amplifier Design*, 3rd ed.; Kendall Hunt Publishing: Dubuque, IA, USA, 2003; pp. 33–62.
- Huang, C.H.; Pawar, S.J.; Hong, Z.J.; Huang, J.H. Insert earphone modeling and measurement by IEC-60711 coupler. *IEEE Trans. Ultrason. Ferroelectr. Freq. Control* **2011**, *58*, 461–469. [[CrossRef](#)] [[PubMed](#)]
- Huang, C.-H.; Pawar, S.J.; Hong, Z.-J.; Huang, J.H. Earbud-type earphone modeling and measurement by head and torso simulator. *Appl. Acoust.* **2012**, *73*, 461–469. [[CrossRef](#)]
- Blanchard, L.; Agerkvist, F. Concha headphones and their coupling to the ear. In Proceedings of the 126th Audio Engineering Society Convention, Munich, Germany, 7–10 May 2009.
- Avis, M.R.; Kelly, L.J. Principles of headphone design—A tutorial review. In Proceedings of the UK 21st Conference: Audio at Home, Cambridge, UK, 6–8 April 2006.
- Tsai, Y.; Shiah, Y.; Huang, J.H. Effects of porous materials in an insert earphone on its frequency response-experiments and simulations. *IEEE Trans. Ultrason. Ferroelectr. Freq. Control* **2012**, *59*, 2537–2547. [[PubMed](#)]

12. Bai, M.R.; Kuo, Y.C. Acoustical design of a bluetooth earphone using simulated annealing optimization. *J. Audio Eng. Soc.* **2010**, *58*, 583–589.
13. Olive, S.; Welti, T.; Khonsaripour, O. The preferred low frequency response of in-ear headphones. In Proceedings of the Audio Engineering Society Conference: 2016 AES International Conference on Headphone Technology, Aalborg, Denmark, 24–26 August 2016.
14. Olive, S.; Welti, T.; Khonsaripour, O. The influence of program material on sound quality ratings of in-ear headphones. In Proceedings of the 142nd Audio Engineering Society Convention, Berlin, Germany, 20–23 May 2017.
15. Kinsler, L.E.; Frey, A.R.; Coppens, A.B.; Sanders, J.V. Fundamentals of acoustics. In *Fundamentals of Acoustics*, 4th ed.; Wiley: Hoboken, NJ, USA, 1999.
16. Slotte, B. Acoustics Simulation in Mobile Phone Audio Design. Master’s Thesis, Science, Helsinki University of Technology, Espoo, Finland, 1999.
17. Nielsen, L.; Schuhmacher, A.; Liu, B.; Jonsson, S. Simulation of the iec 60711 occluded ear simulator. In Proceedings of the 116th Audio Engineering Society Convention, Berlin, Germany, 8–11 May 2004.
18. Jiang, Y.-W.; Kwon, J.-H.; Kim, H.-K.; Hwang, S.-M. Analysis and optimization of micro speaker-box using a passive radiator in portable device. *Arch. Acoust.* **2017**, *42*, 753–760. [[CrossRef](#)]



© 2019 by the authors. Licensee MDPI, Basel, Switzerland. This article is an open access article distributed under the terms and conditions of the Creative Commons Attribution (CC BY) license (<http://creativecommons.org/licenses/by/4.0/>).